Polyelectrolytes Grafted to Curved Surfaces

E. B. Zhulina*

Materials Science and Engineering Department, University of Pittsburgh, Pittsburgh, Pennsylvania 15261

O. V. Borisov

Johannes Gutenberg Universität, Institut für Physik, D-55099 Mainz, Germany

Received October 24, 1995[⊗]

ABSTRACT: We present a scaling theory to describe equilibrium conformations of weakly charged polyelectrolyte molecules grafted at one end onto impermeable surfaces of various morphologies (spheres, cylinders) and of arbitrary curvature. We focus on the case of sufficiently densely grafted chains, i.e., on curved polyelectrolyte brushes. Different regimes of the behavior of curved polyelectrolyte brushes can be distinguished, depending on grafting density, surface curvature, and chain length. We present phase diagrams of the system describing these regimes and discuss the crossover conditions. We also analyze the effect of charge annealing in curved polyelectrolyte brushes.

1. Introduction

The understanding of equilibrium and dynamic properties of monolayers formed by charged polymer chains adsorbed (or grafted) at one end onto solid/liquid or liquid/liquid interfaces of different morphologies is important for numerous technological applications, including development of grafted lubricants and sterically stabilized colloid dispersions and lyposomes and chromatography of proteins and of water-soluble polymers.

Our understanding of the structure and dynamic properties of monolayers formed by end-adsorbed neutral polymer chains (the so-called polymer brushes) is based on scaling and SCF theories and seems to be rather complete (see, for example, a review in ref 1 and references therein).

The same approaches have been applied for the description of monolayers formed by charged polymers (polyelectrolyte brushes) tethered to a planar interface and immersed into a liquid phase.[2−6] As has been shown, the Coulombic interaction between the charges immobilized on the chains causes partial stretching of the grafted polyions in the direction normal to the surface. This stretching is similar to that observed in neutral polymer brushes, but due to the long-range character of Coulombic interactions (in a salt-free solution), the dependences of the brush thickness on the grafting density and on the degree of polymerization of the grafted chains differ from those found for neutral brushes. Moreover, these parameters affect not only the grafted chain conformation (the extension, monomer density profile, etc.) but also the distribution of counterions in the layer and between the layer and the bulk solution.

The problem of counterions distribution becomes even more important for the brushes formed by polyelectrolyte chains grafted onto curved (convex) interfaces. Scaling analysis of an equilibrium structure of spherical and cylindrical polyelectrolyte brushes presented in refs 7−10 concerns the particular case of small curvature radius and large density of grafting (the analysis of spherical micelles with charged coronas presented in refs 11 and 12 refers, actually, to the same limit).

However, for many practical purposes, the dependences of the polyelectrolyte brush structure and of the brush free energy (determining elastic properties) on the radius of curvature of the interface are of particular interest. This problem is of significant importance for the stability of liposomes decorated with grafted polyelectrolytes (see, for example, ref 13).

The aim of this paper is to consider in scaling terms the equilibrium conformations of grafted polyelectrolyte chains and the distribution of counterions between the brush and the solution for spherical and cylindrical (convex) brushes at an arbitrary radius of curvature. We consider polyelectrolytes with quenched (fixed) and annealed (equilibrated) distributions of charge on the grafted chains.

After the description of our model (section 2), we review in short the main results on a quenched planar polyelectrolyte brush (section 3). The equilibrium structure and the counterion distribution for the cases of quenched spherical and cylindrical brushes are considered in sections 4 and 5. In section 6, we discuss the effect of charge annealing in spherical and cylindrical geometries, and we summarize our conclusions in section 7.

2. Model

We consider polyelectrolyte brushes formed by long, weakly charged polyelectrolyte chains grafted at one end onto an impermeable spherical (curvature radius R_s) or cylindrical (curvature radius R_c) surface and immersed into a solvent (Figure 1). The density of grafting is characterized by the surface area s per chain. Let N be the degree of polymerization of every grafted chain and α the fraction of elementary charged monomers, so that the total charge of a grafted polyion is $Q = \alpha Ne$.

We assume the following: (i) The fraction α of charged monomer units is small, $\alpha \ll 1$. For quenched polyelectrolytes, α is a constant and is independent of the system parameters. For annealed polyelectrolytes, the degree of ionization α is not fixed but can vary, adjusting to the variation in external conditions (for example, pH) of the bulk solution. (ii) The Bjerrum length, $l_B = e^2/T\epsilon$, is of the order of a monomer unit length a, and the dimensionless coupling parameter $u = l_B/a$, which characterizes the strength of the Coulombic interaction, is of the order of 1 (here ϵ is the dielectric constant of

[⊗] Abstract published in *Advance ACS Abstracts,* March 1, 1996.

0024-9297/96/2229-2618$12.00/0

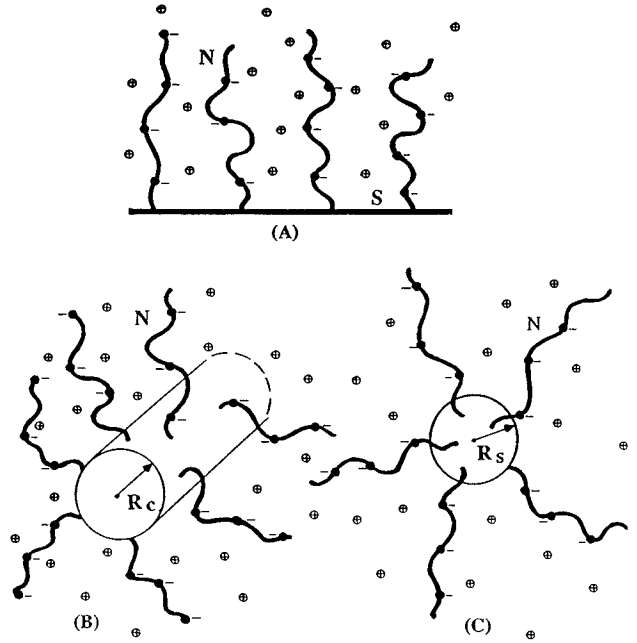

Figure 1. Polyelectrolyte brushes: planar (A), cylindrical (B), and spherical (C).

the solvent and T the temperature in the units of energy). (iii) The nonelectrostatic excluded volume interactions are determined by the ternary contacts between monomers (the vicinity of the θ point for uncharged polymer). (iv) The sphere or the cylinder to which the chains are grafted is localized in the center of a spherical or infinitely long cylindrical shell, respectively. The radius of the shell is much larger than the total radius of the brush (radius of the grafting surface + the brush thickness). The shell contains a solvent (homogeneous dielectric medium) and mobile counterions compensating the brush charge. Thus, the shell is electroneutral as a whole. This approximation corresponds to the conditions of a dilute solution of particles decorated by grafted polyelectrolytes. This solution can contain also small amounts of added ions that determine the pH of the solution.

We shall restrict our consideration to the scaling approximation, neglecting non power dependences and omitting all the numerical coefficients.

3. Polyelectrolyte Brushes of Vanishing Curvature

In this section we summarize the main results on the equilibrium structure of a quenched polyelectrolyte brush in the limit of small curvature of the grafting surface ($R_s \gg H$ or $R_c \gg H$), i.e., the results for a planar polyelectrolyte brush.[2,3,5]

A planar layer of grafted polyelectrolyte chains can be considered as an infinite charged plane characterized by the surface charge density Q/s and the corresponding Guoy−Chapman length λ, which can be interpreted as a characteristic thickness of the counterions cloud above a charged surface,

$$\lambda \cong es/Ql_B \tag{1}$$

In the case of a polyelectrolyte brush, the immobilized charge is not localized on the surface ($x = 0$) but is smeared over a layer of finite thickness, $0 \le x \le H$, above the surface. Here H is the thickness of the brush, the second characteristic length in our system.

According to refs 2 and 5, depending on the ratio H/λ, two qualitatively different regimes of a polyelectrolyte brush behavior can be distinguished:

(1) PBp regime: $H/\lambda \ll 1$. This regime corresponds to a small surface charge density. i.e. small charge of polyions (small α) or small grafting density (large s). As the Guoy−Chapman length is much larger than the thickness of the brush, most of the counterions leave the brush (only a small fraction of them $\sim H/\lambda \ll 1$ penetrate the brush, partially compensating the charge of grafted polyions). The Coulombic force applied to the grafted charged chains, tending to stretch them normally to the surface, can be evaluated using a simple "planar capacitor" model (see ref 5 for details). This force is equal to

$$f_{\text{Coulombic}}/T \cong Q^2a/s \tag{2}$$

per chain. The competition between this stretching force and the elastic force due to chain deformation,

$$f_{\text{el}}/T \cong H/(Na^2) \tag{3}$$

gives the equilibrium chain dimension in the direction normal to the grafting surface (brush thickness),

$$H_{\text{PB}}^{(\text{p})} \cong N^3a^3\alpha^2s^{-1} \tag{4}$$

where subscript PB and superscript p indicate the PBp regime of a planar brush). A strong dependence of the brush thickness on the degree of polymerization of the grafted polyions, $H \sim N^3$, is predicted in this regime.

(2) OsBp regime: $H/\lambda \gg 1$. This regime corresponds to large surface charge density, i.e., to the case when both the grafting density and the charge of every polyion are sufficiently large. Most of the counterions are retained inside the brush by the force of electrostatic attraction to the oppositely charged grafted polyions. The reverse force applied to the polyions and tending to stretch them normally to the grafting surface is proportional to the osmotic pressure of counterions localized inside the brush,

$$f_{\text{osm}}/T \cong \alpha N/H \tag{5}$$

per chain. The balance of this osmotic force with the elastic force given by eq 3 gives the equilibrium brush thickness, which is *independent* of the grafting density:

$$H_{\text{osm}} \cong Na\alpha^{1/2} \tag{6}$$

It should be mentioned that, in the OsB regime, the brush is almost electroneutral as a whole and is electroneutral locally as well: the Debye screening length governed by the mobile counterions inside the brush, $\kappa^{-1} \cong [l_B\alpha N/(sH)]^{1/2}$, is much smaller than the brush thickness H. The fraction of the counterions leaving the brush (the fraction of uncompensated charge) can be estimated as $\sim(\kappa H)^{-1}$.

In both the PBp and the OsBp regimes, grafted polyelectrolyte chains are partially stretched normally to the grafting surface. They can be presented as completely stretched chains of Pincus blobs[14] (parts of the chains retaining unperturbed Gaussian conformation), formed by the stretching forces, $f_{\text{Coulombic}}$ and f_{osm}, respectively. In the OsBp regime, the number of blobs per chain is determined by the condition "one charge per blob"; i.e., the blob size is equal to $\xi_{\text{osm}} \cong a\alpha^{-1/2}$. In the PBp regime, the size of the stretching blob is given

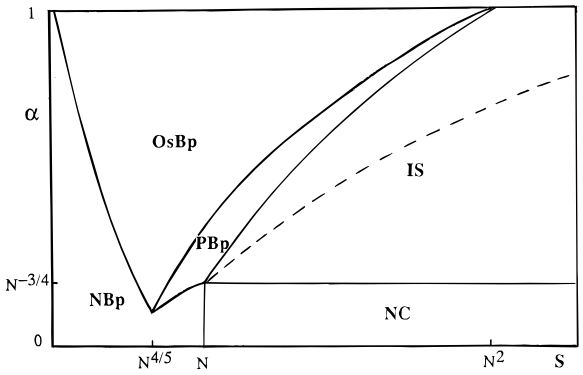

Figure 2. Diagram of states of a planar polyelectrolyte brush in α,*s* coordinates.

by $\xi_{PB} \cong T/f_{Coulombic} \cong s/aQ^2$, and each blob has more than one charge. Note that, in contrast to the blob picture of a neutral polymer brush,[15,16] the blobs in a polyelectrolyte brush are not closely packed.

A third important regime of polyelectrolyte brush behavior is the quasineutral NBp regime, which occurs at sufficiently large grafting density but at small fraction of charged monomers in the grafted polyions. In this case, the nonelectrostatic interactions between the uncharged monomers in the grafted chains predominate over the electrostatic interactions, and the layer acquires a structure of a neutral polymer brush with the thickness

$$H_n^{(p)} \cong Na(s/a^2)^{-1/2} \tag{7}$$

The above expression for H corresponds to Θ solvent conditions when the stretching of the grafted chains is caused by the ternary intermonomer interactions, with the third virial coefficient of the order of 1.[25] The crossover between the polyelectrolyte regimes, PBp and OsB, and the quasineutral regime, NBp, can be determined by the condition of close packing of Pincus blobs.

It should be mentioned that, in the framework of the scaling approximation used here, a planar polyelectrolyte brush in all the described regimes is characterized by a constant density of monomers. The more sophisticated SCF approach[4] shows that the monomer density decreases monotonically from the grafting surface to the edge of the brush. However, this decrease is described by a non power function that corresponds to a stepwise density profile in the scaling approximation.

In the diagram of states of a planar polyelectrolyte brush presented in Figure 2 in α,*s* coordinates, in addition to the brush regimes PBp, OsBp, and NBp described above, the two nonbrush or "mushroom" regimes (regimes of weakly interacting, sparsely grafted polyions) can be found: the NC regime of quasineutral Gaussian coils unperturbed by intra- or intermolecular interactions (if $\alpha \ll N^{-3/4}$) and the IS regime of individual grafted polyions stretched by intramolecular Coulombic repulsion (if $\alpha \gg N^{-3/4}$). The size of individual polyions in the latter regime is equal to $R_0 \cong Na\alpha^{2/3}(l_B/a)^{1/3}$.[17,18] The boundary between the PBp and the IS regimes corresponds to the overlap condition, $s \cong R_0^2$. The boundary between the NBp and the NC regimes is given by the condition $s \cong Na^2$. In the part of the IS region between the dashed line and the IS/PBp boundary, the Coulombic interactions between the grafted chains cause noticeable orientation of the polyions normally to the surface (see ref 5 for discussion).

4. Cylindrical Polyelectrolyte Brush

In this section we consider a cylindrical brush or a "bottle-brush" formed by polyelectrolyte chains grafted at one end onto an infinitely long cylinder. The brush is immersed into an infinitely long cylindrical shell of radius exceeding by far the maximal brush thickness. It is convenient to introduce an axial separation between the grafted chains (inverse linear grafting density), $h \cong s/R_c$, and the corresponding linear charge density, $q = Q/h$, created by the grafted polyions.

4.1. Thin Cylinder. Let us start with the case of a thin cylinder, where the radius of the cylinder is much smaller than the dimension of grafted polyions in the direction perpendicular to the axis of the cylinder, $R_c \ll H$.

Let the fraction of charged monomer in every chain be large enough, $\alpha \gg N^{-3/4}$, that an individual polyion is stretched by intramolecular Coulombic repulsion.

If the axial separation h exceeds the dimension of an individual polyion in the solution R_0, then the grafted polyions retain, in general, the same conformation as in the dilute solution.

It is known that if $Q/h \ll l_B^{-1}$, then all the counterions are "free", i.e., are spread all over the volume of the shell (the characteristic scale of the decay of counterion density with a distance from the cylinders is larger than the radius of the shell).

The electrical field created by grafted polyions at the distance $r \geq H$ from the surface is given by $e\Psi(r)/T \cong l_B(\alpha N/h) \ln r$. The electrostatic force applied to each grafted polyion and acting in the radial direction is equal to

$$f_{Coulombic}/T \cong l_B(\alpha N)^2(hH)^{-1} \tag{8}$$

It is easy to see that if $R_0 \ll h$, this force remains much weaker than the intramolecular Coulombic repulsion force, Q^2/R_0^2, and is thus unable to cause additional stretching of the grafted chains.

However, in the range $R_0 \ll h \ll (\alpha N)^2 l_B$, the condition $f_{Coulombic}R_0/T \geq 1$ is fulfilled, and the intramolecular Coulombic repulsion leads to orientation of the grafted polyions in the radial direction.

The averaged monomer density decreases in the radial direction as $c(r) \sim r^{-1}$.[19]

At $h \leq R_0$, i.e., above the conventional overlap threshold,[20] the electrostatic force $f_{Coulombic}$ given by eq 8 becomes stronger than the intramolecular stretching force, Q^2/R_0^2. A competition of the elastic force given by eq 3 and the electrostatic force given by eq 8 results in a new dependence for the brush thickness,

$$H_{PB}^{(c)} \cong N^{3/2}a\alpha(l_B/h)^{1/2} \tag{9}$$

where subscript PB and superscript c indicate the regime of strong charge separation in a cylindrical brush). Thus, the polyelectrolyte bottle-brush thickness increases with a decrease in the axial chains separation as $H \sim h^{-1/2}$.

A decrease in the axial separation between the grafted chains, h, leads to a simultaneous increase in the linear charge density, $q = Q/h$. At $h \leq Ql_B/e$, the Manning condensation of counterions on a cylindrical bottle-brush starts. Although an exact solution of the Poisson–Boltzmann equation for counterions distribution in the case of a permeable charged cylindrical layer is not available, we assume in the framework of our approximation that a "condensed" fraction of the counter-

ions, $\phi = 1 - eh/(l_B Q)$, is localized at $0 \le r \le H$, i.e., inside the bottle-brush. Hence, at $Q/(eh) \ge l_B^{-1}$, the effective (uncompensated) charge per unit length of the bottle-brush is equal to $Q^*/h \cong e/l_B \ll Q/h$. Correspondingly, at $h \ll Ql_B/e$, most of the counterions are localized inside the bottle-brush, which is almost electroneutral as a whole and electroneutral locally as well ($\kappa H \gg 1$, where $\kappa^2 \cong l_B \alpha N/(H^2 h)$).

This "osmotic" regime is equivalent, of course, to the OsB regime in the planar polyelectrolyte brush.

The stretching force applied to the grafted polyions is determined in this regime by the osmotic pressure of the counterions inside the bottle-brush, $f_{osm} \cong \alpha N/H$ (per chain). As this force coincides (within scaling approximation) with that given by eq 5 for a planar brush, the thickness of the bottle-brush in the osmotic OsBc regime is still given by eq 6 and is thus independent of the brush morphology and the grafting density.

The chains in a polyelectrolyte bottle-brush stretched in the osmotic regime can be also envisioned as chains of "osmotic" Pincus blobs of constant size, $\xi_{osm} \cong a\alpha^{-1/2}$, which is independent of the brush morphology as well.

Since the chains in a bottle polyelectrolyte brush in the OsBc regime are stretched radially in proportion to their contour length, N, the monomer density must decay with a distance, r, from the axis proportionally to r^{-1},

$$c_{osm}^{(c)}(r) \cong (ah\alpha^{1/2}r)^{-1} \tag{10}$$

As the axial separation between grafted polyions, h, decreases further, there are two scenarios depending on the fraction of charged monomers: (i) if the chains are charged sufficiently strongly, $\alpha \gg N^{-2/3}$, then the OsBc regime occurs up to the limiting high grafting density, $h \le a$; (ii) if the fraction of charged monomers is small enough, $\alpha \ll N^{-2/3}$, then the nonelectrostatic short range interactions (ternary repulsion) between the uncharged monomers predominates over osmotic pressure of the counterions at small h. The polyelectrolyte bottle-brush acquires the structure of a neutral one with thickness[21]

$$H_n^{(c)} \cong N^{2/3}a(a/h)^{1/3} \tag{11}$$

where subscript n and superscript c denote the neutral cylindrical brush regime, whereas the radial decay of the monomer density is given by

$$c_n^{(c)}(r) \cong (rh)^{-1/2}a^{-2} \tag{12}$$

Such a brush can be presented as a system of densely packed concentrational blobs growing in the radial direction, $\xi_n^{(c)}(r) \cong (rh)^{1/2}$. The crossover between the osmotic and the quasineutral regimes occurs at $\xi_{osm}^{(c)} \cong \xi_n^{(c)}$, where the size of the concentrational blob is taken at the edge of a brush.

The diagram of states of a polyelectrolyte bottle-brush at $R_c \ll H$ is presented in Figure 3 in α,h coordinates. We see that, qualitatively, it is similar to the corresponding diagram for a planar polyelectrolyte brush, i.e., it contains three brush regimes (the osmotic regime, OsB_c, the regime of unscreened Coulombic interaction in the brush, PB_c, and the regime of dominance of nonelectrostatic interactions, NB_c) as well as the regimes of weakly interacting polyions (IS) and Gaussian coils unperturbed by intramolecular Coulombic interactions (NC).

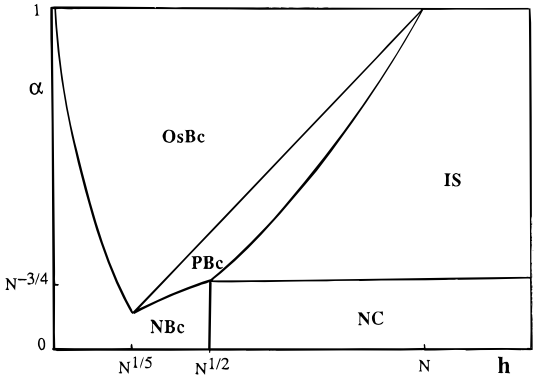

Figure 3. Diagram of states of a cylindrical (bottle) brush in α,h coordinates.

4.2. Bending a Planar Brush into a Cylinder. So far we have considered different regimes of the behavior of a polyelectrolyte bottle-brush at different axial separation between grafted chains and different fractions of charged monomers at constant (small) radius of the grafting surface.

Let us consider now the dependence of the brush structure and counterions distribution on the radius of the cylinder, R_c, assuming that the surface area per grafted chain is fixed.

It is obvious that, when the radius, R_c, exceeds by far the thickness of the brush, H, the brush structure coincides in general with that of a planar brush with the same density of grafting (with the same s).

The succession of different regimes through which the brush passes as the radius, R_c, decreases depends on the surface grafting density, s^{-1}, and the fraction of charged monomers, α. The diagrams of state of a cylindrical polyelectrolyte brush in α,R_c coordinates presented in Figure 4 describe the changes in the brush structure in various ranges of s values.

If the chains in the brush are grafted sufficiently densely ($s \ll N^{4/5}a^2$, Figure 4A), then at $1/R_c \to 0$, the brush is found either in the OsBp or in the NBp regime. The brush thickness is given by eqs 6 and 7 at $\alpha \gg a^2/s$ and $\alpha \ll a^2/s$, respectively. A decrease in the radius, R_c, does not affect significantly the chains conformation and the counterions distribution until R_c remains larger than the brush thickness, H. Here the stretching of the grafted chains becomes weaker but in nonscaling terms.

However, at $R_c \le H$, the effect of curvature becomes significant, and the brush passes to the OsBc or to the NBc regime.

At $\alpha \gg (s/a^2)^{-1}$, the polyelectrolyte cylindrical brush continues to retain its counterions, and the brush thickness is still given by eq 6 (a decrease in H accompanying the decrease in R_c has the character of a non power dependence). Further decrease in R_c results, however, in a decrease in the value of the charge per unit length of the cylinder. As a result, at $\alpha \ll s(R_cN)^{-1}$, the counterions leave the internal region of the bottle-brush and spread all over the volume of the solution. The interaction between the grafted polyions acquires the character of unscreened Coulombic repulsion, and the brush passes into the PBc regime. Correspondingly, the brush thickness starts to decrease with a decrease in R_c as $H_{PB}^{(c)} \cong R_c^{1/2}N^{3/2}al_B^{1/2}\alpha s^{-1/2}$. Further decrease in R_c results in the decomposition of the bottle-brush into separate mushrooms, which either are stretched by intramolecular Coulombic repulsion (if $\alpha \gg N^{-3/4}$) or are Gaussian (if $\alpha \ll N^{-3/4}$). In the former case, the bottle-brush passes through the NBc regime, too. In the

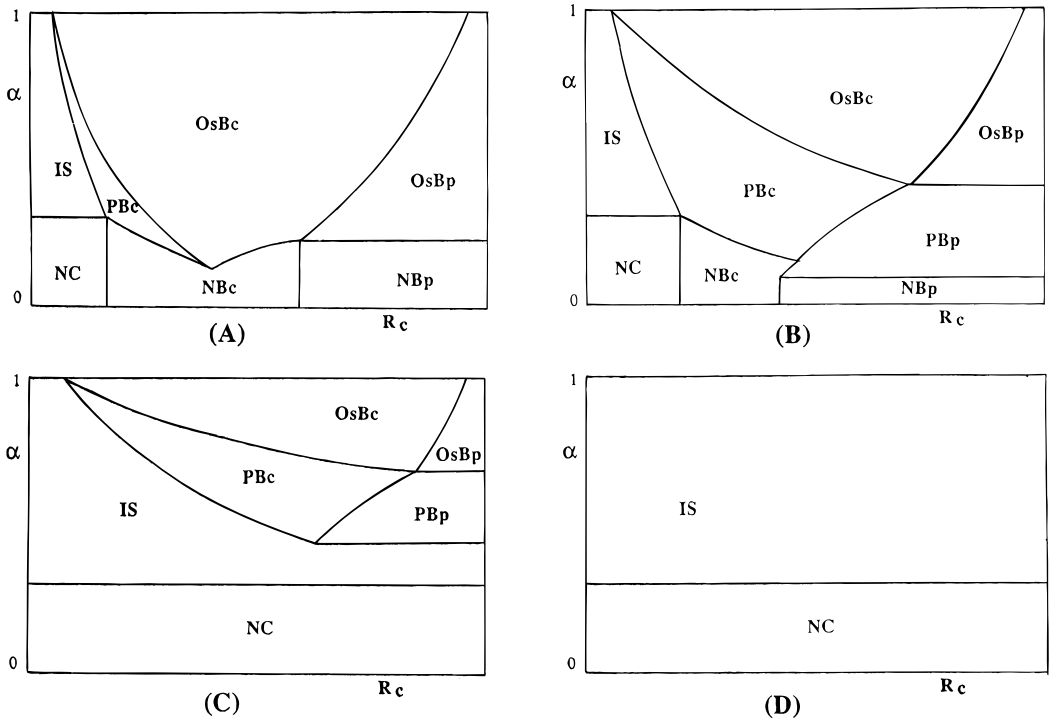

Figure 4. Diagrams of states of the bent cylindrical brushes in α,R_c coordinates for various ranges of s: $s/a^2 \ll N^{4/5}$ (A), $N^{4/5} \ll s/a^2 \ll N$ (B), $N \ll s/a^2 \ll N^2$ (C), and $s/a^2 \gg N^2$ (D).

latter case ($\alpha \ll (s/a^2)^{-1}$), the brush thickness starts to decrease with a decrease in R_c at $R_c \leq H_n^{(p)}$, i.e., just after crossing the boundary of the NBc regime, $H_n^{(c)} \cong N^{2/3}aR_c^{1/3}(s/a^2)^{-1/3}$. Finally, a decrease in R_c results in a decomposition of the bottle-brush into Gaussian mushrooms grafted onto the cylinder. However, if $N^{-4/5} \ll \alpha\ (s/a^2)^{-1}$, a decrease in R_c, leading to a decrease in the linear charge density $q = QR_c/s$, results first in the dominance of the counterions' osmotic pressure over the nonelectrostatic interactions (OsBc regime) and then in the loss of the counterions and predominance of the Coulombic repulsion (PBc regime), and finally, when the charge density becomes small enough, the nonelectrostatic interactions become dominant again (NBc regime).

The diagrams corresponding to other ranges of s are presented in Figure 4B−D.

5. Spherical Polyelectrolyte Brush

In this section we describe the structure of a spherical polyelectrolyte brush formed by polyelectrolyte chains grafted onto a spherical surface of radius R_s and immersed in a spherical shell of solvent. The outer radius of the shell is assumed to be much larger than $R_s + H$, and we consider the situations corresponding to different ratios of R_s and the brush (the "corona") thickness, H.

5.1. Small Sphere. We start our consideration with the case of a small radius of the sphere, $R_s \ll H$. This system has been treated in refs 2, 7−10, some relevant results concerning spherical micelles with charged coronas were obtained in refs 11 and 12; and the systematic study of a polyelectrolyte star (which can be considered as a spherical polyelectrolyte brush with $R_s = 0$) has been performed recently.[22]

In Figure 5, we present the diagram of states of a spherical polyelectrolyte brush in α,s coordinates for the case $R_s \ll N^{1/2}a$. As the radius of the grafting sphere is

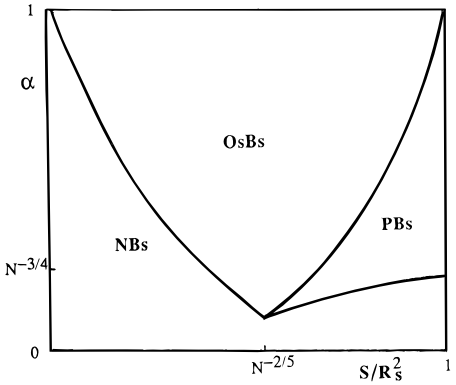

Figure 5. Diagram of states of a spherical brush in $\alpha,s/R_s^2$ coordinates.

fixed, the variation in s (area per grafted chain) leads to variation in the total number, R_s^2/s, of the grafted chains.

The diagram of states contains three regions. The PBs regime corresponds to a small number of sufficiently strongly charged chains grafted onto the sphere. In this case, the total charge of the corona, QR_s^2/s, is not large enough to keep the counterions, which leave the brush and spread all over the volume of the shell. Thus, the polyions in the brush interact via the unscreened Coulombic potential, and the electrostatic force applied to each chain, tending to stretch it radially, is given by $f_{Coulombic}/T \cong R_s^2 l_B(\alpha N)^2/H^2 s$. Balance of this force and the chain elasticity, eq 3, gives the radial dimension of the grafted chains,

$$H_{PB}^{(s)} \cong Na\alpha^{2/3}(R_s^2/s)^{1/3}(l_B/a)^{1/3} \qquad (13)$$

where subscript PB and superscript s indicate the PB regime of a spherical brush. As the surface area per chain, s, decreases, the thickness of the corona, $H_{PB}^{(s)}$, increases. However, as follows from eq 13, it increases more slowly than the total charge of the corona,

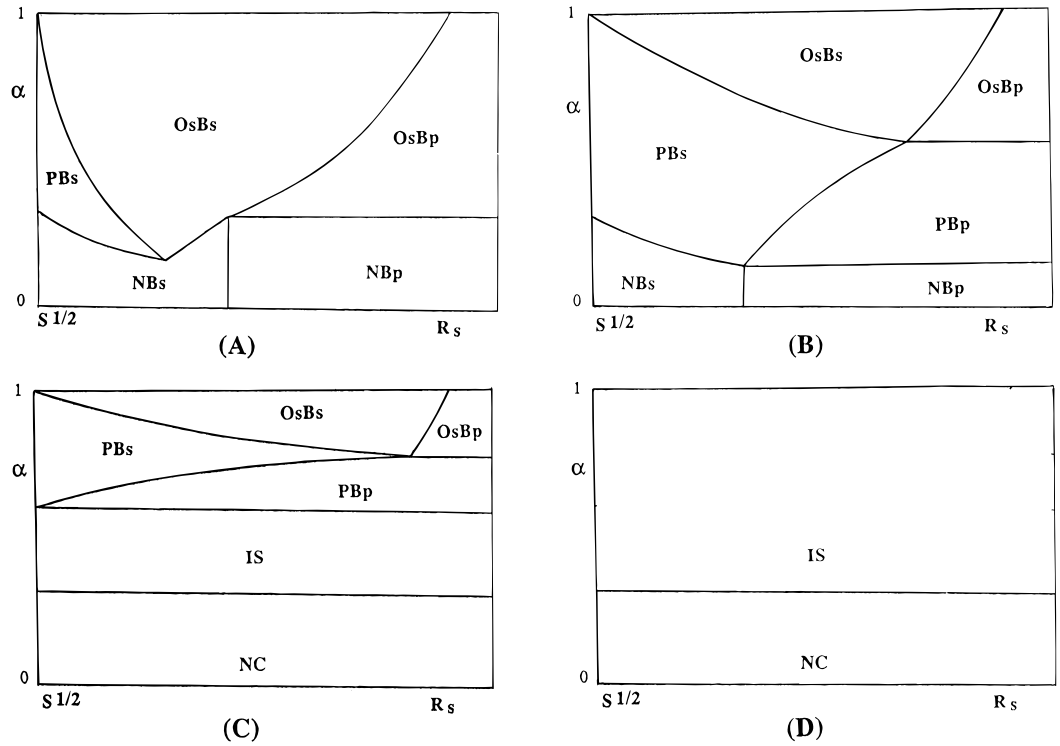

Figure 6. Diagrams of states of the bent spherical brushes in α,R_s coordinates for the same ranges of s as in Figure 4.

QR_s^2/s. As a result, at $QR_s^2/es \geq H/l_B$ ($s \ll s^*$, where $s^* \cong R_s^2\alpha^{1/2}(l_B/a)$), a significant redistribution of counterions occurs. Most of the counterions penetrate the corona region, almost compensating its charge. This effect of charge renormalization has been described for charged spherical particles in ref 23 and discussed in different aspects for spherical polyelectrolyte brushes, micelles, and stars in refs 2, 11, and 22. At $s \leq s^*$, the effective (uncompensated) charge of the corona is equal to eH/l_B, which is much smaller than its bare charge, QR_s^2/s. The equilibrium radius of the corona, H, is determined now by the balance between the osmotic pressure of the counterions inside the corona (still given by eq 5) and the conformational elasticity of the chains. Thus, at $s \leq s^*$, the spherical polyelectrolyte brush is found in the osmotic regime OsBs, and its thickness (radial chains dimension) is given by the conventional dependence, $H_{osm}^{(s)} \cong Na\alpha^{1/2}$.

Since the chains in the corona are stretched in proportion to their contour length, the monomer density decreases in the radial direction as

$$c_{osm}^{(s)}(r) \cong [NR_s^2/(sH)]r^{-2} \cong [\alpha^{1/2}R_s^2/s]r^{-2} \quad (14)$$

This monomer density profile corresponds to presentation of each chain in the corona as a sequence of Pincus stretching blobs of constant size, $\xi_{osm}^{(s)} \cong a\alpha^{-1/2}$.

In the osmotic regime, an increase in the number of chains grafted onto a sphere (a decrease in s) does not lead to the growth of the corona size but gives rise to the monomer concentration in the corona. As a result, at sufficiently small values of s, the nonelectrostatic interactions between the uncharged monomers start to play an important role and compete with the osmotic pressure of the counterions. At $s \ll s^{**} \cong (R_s/(\alpha N))^2$, these interactions determine the structure of the corona, and its thickness starts to grow again with a decrease in s according to refs 24 and 25,

$$H_n^{(s)} \cong N^{1/2}a(R_s^2/s)^{1/4} \quad (15)$$

Here the brush can be envisioned as a densly packed system of blobs with increasing size, $\xi(r) \cong (R_s^2/s)^{-1/2}r$. Correspondingly, the profile of density of monomer units is given by

$$c_n^{(s)} \cong (R_s^2/s)^{1/2}r^{-1} \quad (16)$$

The diagram in Figure 5 comprises the three brush regimes discussed above. The mushrooms regimes, which are found for cylindrical and planar geometries, collapse into a single vertical line, $s/R_s^2 \cong 1$.

5.2. Bending a Planar Brush into a Sphere. Let us consider now how the brush structure and the counterions distribution depend on the radius of the sphere, R_s, assuming that the area per chain, s, is fixed constant. Similarly to the case of the cylindrical brush, at $R_s \gg H$, the brush structure is only slightly affected by the variation in R_s. The succession of various regimes that the brush passes with decreasing $R_s < H$ depends on the values of s and α. The picture is qualitatively similar to that for cylindrical brushes. At relatively dense grafting, $s \ll a^2N^{4/5}$ (Figure 6A), the brush is found either in the regimes of planar behavior (OsBp and NBp) at high values of $R_s \gg H$ or in the regimes of a spherical brush (OsBs, PBs, and NBs) at $R_s \ll H$. The boundaries $R_s \cong aN\alpha^{1/2}$ and $R_s \cong aN(s/a^2)^{-1/2}$ separate the spherical regimes from the planar regimes for strongly charged ($\alpha \gg a^2/s$) and weakly charged ($\alpha \ll a^2/s$) brushes, respectively. Decreasing R_s leads to the diminishing of the total number of the grafted polyions and, thus, a decrease in the total charge of the brush QR_s^2/s. The electrostatic attraction between the grafted polyions and mobile counterions also decreases, and the mobile ions start to leave the brush. This effect becomes essential at $H_{osm}^{(s)} \cong QR_s^2/s$, to give the boundary between the OsBs and the PBs regimes, $\alpha \cong s^2/R_s^4$. To the left of this boundary (inside the PBs

regime), only a small fraction of all the counterions is found inside the brush, and the chains are barely charged. This regime retains until $R_s \cong (s/a^2)^{1/2}$, i.e., until there is one charged polyion grafted onto a sphere. Decreasing α at small values of R_s leads to the transition from the PBs regime into the regime of quasineutral behavior, NBs. The boundary between the two regimes is determined by the condition $H_{PB}^{(s)} \cong H_n^{(s)}$, to give $\alpha \cong (s/R_s^2)^{1/8}N^{-3/4}$. The boundary between the NBs and the OsBs regimes found at higher values of R_s is given by the condition $H_n^{(s)} \cong H_{osm}^{(s)}$, to give $\alpha \cong (R_s^2/s)^{1/2}N^{-1}$.

The diagrams corresponding to the other ranges of s are presented at Figure 6B−D. The boundaries between the different regimes can be obtained by equating the corresponding expressions for the brush thickness in any two neighboring regions.

6. Effect of Charge Annealing in Spherical and Cylindrical Brushes

All the above results were obtained at a fixed value of α, i.e., for quenched polyelectrolytes. However, charge annealing is known to induce new and interesting features in the brush behavior. So far, the annealing effects were considered only for planar geometry of polyelectrolyte brushes.[6,26−28] As was demonstrated in ref 6, charge annealing can lead to "abnormal" behavior of a polyelectrolyte brush, i.e., an increase of the brush thickness with increasing area per chain, s, and/or increasing the ionic strength of the solution. The effects are most pronounced at low ionic strengths of solution (salt-free solutions). Manifestation of the annealing effects is expected to be noticeable in the curved polyelectrolyte brushes as well. In the remaining part of this paper, we focus on the annealing charge effects in cylindrical and spherical brushes in the OsB regimes.

6.1. Annealed Polyelectrolytes. We consider now polyelectrolytes with the degree of ionization, α, adjusting to the local environment of the grafted chains. A typical example of such a polyelectrolyte is a weak acid homopolymer. In such a chain, each monomer can dissociate, and the average degree of chain ionization, α (average fraction of charged monomers), is determined by the mass action law,

$$\alpha/(1-\alpha) = K/c_H \tag{17}$$

Here, c_H is the local concentration of the protons in the brush, whereas K is the dissociation constant, which is assumed to be independent of both α and c_H. The degree of ionization of an acid group in the bulk solution (i.e., outside the brush), α_b, is determined by the bulk concentration of protons $c_H^{(bulk)} = -\log$ pH,

$$\alpha_b/(1-\alpha_b) = K/c_H^{(bulk)} \tag{18}$$

The main difference between the quenched and the annealed polyelectrolytes is related to the dependence of α in the annealed case on various parameters of the system, such as s, pH, ionic strength of the bulk solution, etc. Moreover, as we show below, the annealing effects in curved brushes lead to an inhomogeneous charging of the grafted chains, i.e., the local degree of chain charging becomes a function of the distance, r, from the grafting surface.

6.2. Monomer Density Profiles in Annealed Brushes. As follows from the results of sections 4 and 5, one can represent the profiles of polymer units in all the OsB regimes of the quenched brushes (indicated by subscript q) in the form of universal dependence,

$$c_q^{(d)}(r) \cong a^{-3}[\sigma_d/\alpha^{1/2}](a/r)^{d-1} \tag{19}$$

Here d is the effective dimensionality of chains in the brush (d = 1, 2, and 3, corresponding to planar (p), cylindrical (c), and spherical (s) brushes respectively), and σ_d is the corresponding dimensionless grafting density of the chains,

$$\sigma_1 = a^2/s \qquad \sigma_2 = a/h = aR_c/s \qquad \sigma_3 = R_s^2/s \tag{20}$$

The dependence described by eq 19 determines the distribution of polymer units and the corresponding blob size, $\xi_d \cong a\alpha^{-1/2}$, throughout the brushes under the conditions

$$\xi_d < s^{1/2} \tag{21}$$

When the above inequality is violated, a planar brush is found in the quasineutral regime NBp, whereas cylindrical and spherical brushes have an internal sublayer with quasineutral distribution of polymer units, eqs 12 and 16. Using the notations of eq 20, one can also represent the dependences of eqs 12 and 16 for the profiles in quasineutral regimes in the universal form,

$$c_n^{(d)}(r) \cong \sigma_d{}^{1/2}(a/r)^{(d-1)/2}a^{-3} \tag{22}$$

The thickness of the internal sublayer, ρ_q, can be determined from the condition

$$c_q^{(d)}(\rho_q) = c_n^{(d)}(\rho_q) \tag{23}$$

to give

$$\rho_q \cong a(\sigma_d/\alpha)^{1/(d-1)} \tag{24}$$

The thickness of the sublayer, ρ_q, is thus independent of the molecular weight of the grafted chains, and for sufficiently long chains, one finds the dependence of eq 19 for the profile, at least in the periphery parts of the curved layers.

The monomer density distribution (eq 19), together with eqs 17 and 18, provides an opportunity to find the monomer density profiles in annealed cylindrical and spherical brushes. In the OsB regimes (counterions localized inside the brushes), the condition of local electroneutrality determines the profile of the mobile counterions (H^+ ions),

$$c_H(r) \approx \alpha(r)c_a^{(d)}(r) \cong a^{-3}\alpha^{1/2}(r)\sigma_d(a/r)^{d-1} \tag{25}$$

where subscript a indicates an annealed brush. Substituting eq 25 into eq 24, one gets an equation for the profile for the degree of chain ionization, $\alpha(r)$,

$$\alpha^{3/2}(r)/(1-\alpha(r)) = Ka^3\sigma_d{}^{-1}(r/a)^{d-1} \tag{26}$$

At $\alpha \ll 1$, eq 26 gives the power asymptotical dependence for the profile of ionization,

$$\alpha(r) \cong (Ka^3/\sigma_d)^{2/3}(r/a)^{2(d-1)/3} \tag{27}$$

Substituting eq 27 into eq 25, one arrives at the profile of monomer units density in annealed brushes of various geometries,

$$c_a^{(d)}(r) \cong a^{-2}\sigma_d^{4/3}K^{-1/3}(a/r)^{4(d-1)/3} \quad (28)$$

At $d = 1$ (planar brush), eq 28 recovers the earlier result,[6] whereas at $d = 2$ (cylindrical brush) and $d = 3$ (spherical brush), one gets new scaling dependences for the profiles of polymer units. Due to the charge annealing, one finds a more rapid radial decay in the concentration of polymer units with respect to quenched systems with $\alpha = \alpha_b$. It should be noted that, similarly to the case of quenched systems, internal parts of the curved annealed brushes can be found under the conditions of a quasineutral behavior (eq 22 for monomer density profiles). The thickness of the internal sublayer, ρ_a, can be obtained from eq 24, taking into account the interconnection between α and r through eq 27. This gives

$$\rho_a \cong a\sigma_d^{1/(d-1)}/(Ka^3)^{2/5(d-1)} \quad (29)$$

Typically, $\rho_a \gg \rho_q$, indicating noticeable weakening of the electrostatic interactions in the annealed systems (spreading of the zone of quasineutral behavior to the outer parts of the brushes). Within these zones, the local degree of chain ionization, α, is still determined by the mass action law, eq 17. Here the concentration of protons $c_H \approx \alpha c_n^{(d)}(r)$, and at $\alpha \ll 1$, one gets

$$\alpha(r) \approx (K/c_n^{(d)}(r))^{1/2} \cong (Ka^3)^{1/2}\sigma_d^{-1/4}(r/a)^{(d-1)/4} \quad (30)$$

Thus, at $r \ll \rho_a$ the profile of the brush ionization is given by eq 30, whereas at $r \gg \rho_a$, eq 27 is appropriate. As is seen from eqs 27 and 30, $\alpha(r)$ is an increasing function of r, so the periphery parts of the brushes are more strongly charged than the internal parts. Since the degree of chain ionization cannot exceed its bulk value, $\alpha_b \approx K/c_H^{bulk}$, one finds a second length scale which restricts the range of applicability of eq 28 from above,

$$\rho_a' \cong a(Ka^3)^{2/(d-1)}(c_H^{(bulk)})^{-4/(d-1)}\sigma_d^{1/(d-1)} \quad (31)$$

At $r \cong \rho_a'$ the local concentration of H^+ ions in the brush reaches its bulk value, $c_H(\rho_a') \approx c_H^{bulk}$, and at $r \gg \rho_a'$, the degree of ionization $\alpha(r) \approx \alpha_b$. At $r \gg \rho_a'$, the electrostatic interactions between charged monomers can be described by the effective second virial coefficient,

$$v_{eff} \cong \alpha_b^2/c_H^{bulk} \cong K^2/(c_H^{bulk})^3 \quad (32)$$

similarly to the situation in a salt dominance regime.[5] Here, the distribution of polymer units is similar to that in a corresponding neutral system under a good solvent conditions ($v_{eff} > 0$). However, for realistic values of N and c_H^{bulk} and in salt-free solutions, ρ_a' exceeds the brush thickness, H, by far, and we do not discuss this regime in the present publication.

Figure 7 presents the blob pictures of curved brushes for the quenched and the annealed cases. In both quenched and annealed systems, the internal part of the brush is found in the quasineutral regime (at $r < \rho_a$ and $r < \rho_q$, the blobs are densly packed and increase in size). At $r > \rho_q$ (quenched case, Figure 7a), the blobs have constant size, $\xi \cong a\alpha^{-1/2}$, and there is one charge per blob. Here, the blobs do not densely fill the space as in the quasineutral sublayer. For an annealed system (Figure 7b), at $r > \rho_a$, the rule "one charge per blob" remains valid as well. However, due to an increase in α to the periphery of the brush (eq 27), the size of the blobs, $\xi \cong a\alpha(r)^{-1/2} \cong a(Ka^3/\sigma_d)^{-1/3}(r/a)^{-(d-1)/3}$, diminishes with increasing r. In both quenched and annealed brushes, the chains of blobs fluctuate in lateral dimensions (dashed lines in Figure 7 indicate some "average" conformation of the grafted polyions).

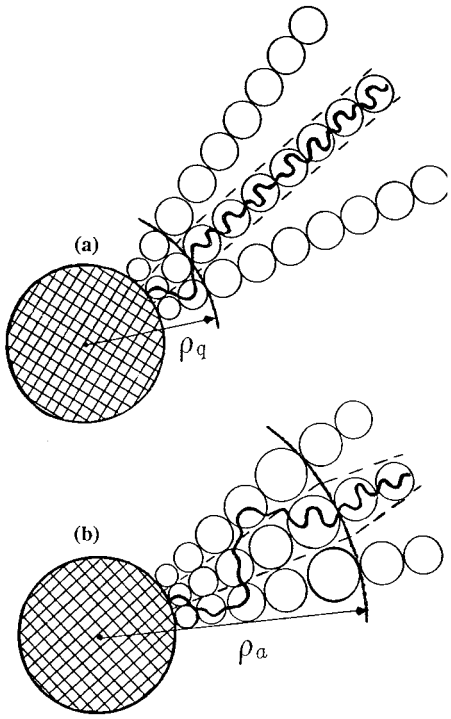

Figure 7. Blob picture of a quenched (a) and an annealed (b) spherical or cylindrical brush in the OsB regimes.

6.3. Dimensions of Annealed Brushes. The distributions of monomer units (eq 28) determine the averaged dimensions, H_a, of the annealed brushes in osmotic regimes. Using normalization conditions for the density profiles,

$$N = \int_0^{H_a} c_a^{(d)}(r) r^{(d-1)} \sigma_d^{-1} a^{3-d}\, dr \quad (33)$$

one gets for the brush thickness,

$$H_a \cong a[N(Ka^3)^{1/3}\sigma_d^{-1/3}]^{3/(4-d)} \quad (34)$$

At $d = 1$ (planar brush), eq 34 recovers the earlier result,[6]

$$H_a \cong aN(Kas)^{1/3} \quad (35)$$

At $d = 2$ (cylindrical, bottle-brush), one has

$$H_a \cong aN^{3/2}(Kas/R_c)^{1/2} \quad (36)$$

where at $d = 3$ (spherical brush),

$$H_a \cong aN^3(Ka^3)s/R_s^2 \quad (37)$$

Note that, for quenched brushes, $H_q \cong aN\alpha^{1/2}$ for all the geometries. As is seen from eqs 35−37, one finds the "abnormal" type of behavior in the annealed brushes in all considered cases; i.e., the brush thickness increases with decreasing the grafting density. The origin of this effect is the same for planar and curved brushes. Looser brushes conserve fewer counterions, and their average

degree of ionization is thus higher than that for more dense brushes.

7. Conclusions

The diagrams in Figures 3−6 demonstrate that bending a planar brush into a cylinder or sphere does not lead to the appearance of physically new regimes. In both cases, one finds the regimes of quasineutral behavior at low values of α (NBp, NBc, and NBs), the regimes of barely charged brush (PBp, PBc, and PBs), and the osmotic brush regimes with condensed counterions (OsBp, OsBc, and OsBs) at high values of α. The geometry of the surface affects the values of the exponents in the PB and NB regimes, whereas in the OsB regimes, one finds a universal expression for the brush thickness, independent of the brush morphology. Diagrams also indicate that the osmotic regimes occupy a major part of the parameter's space, whereas the PB regimes are rather narrow in all geometries.

The effect of annealing the charge on the grafted polyions leads to an unusual, nonmonotonic dependence of the brush thickness on the grafting density in all three geometries. At small grafting density (corresponding to the conditions of the PB regime), the brush thickness increases with σ_d increasing due to the unscreened Coulombic repulsion between grafted polyions. Further increase in σ_d results in decreasing brush thickness due to recombination of the counterions (a decrease in the local and average degrees of chain ionization). However, at sufficiently large grafting density, nonelectrostatic interactions come into play, and the thickness of the brush starts to increase again.

The monomer density in annealed curved polyelectrolyte brushes decreases with the distance from the grafting surface more rapidly than that in quenched brushes. The reason for this is the radial growth of the local degree of chains ionization and, as a result, a slower radial decrease in local chain stretching than in quenched brushes.

Acknowledgment. O.V.B. appreciates the hospitality of Prof. K. Binder, Johannes Gutenberg Universität, Mainz, and the financial support of the Alexander von Humboldt Foundation. E.B.Z. acknowledges the hospitality of Prof. A. C. Balazs at the University of Pittsburgh and the financial support from the Materials Research Center, funded by AFOSR, through Grant No. F49620-95-1-0167.

References and Notes

(1) Halperin, A.; Tirrell, M.; Lodge, T. P. *Adv. Polym. Sci.* **1992**, *100*, 31.
(2) Pincus, P. A. *Macromolecules* **1991**, *24*, 2912.
(3) Borisov, O. V.; Birshtein, T. M.; Zhulina, E. B. *J. Phys. II* **1991**, *1*, 521.
(4) Zhulina, E. B.; Borisov, O. V.; Birshtein, T. M. *J. Phys. II* **1992**, *2*, 63.
(5) Borisov, O. V.; Zhulina, E. B.; Birshtein, T. M. *Macromolecules* **1994**, *27*, 4795.
(6) Zhulina, E. B.; Birshtein, T. M.; Borisov, O. V. *Macromolecules* **1995**, *28*, 1491.
(7) Ross, R.; Pincus, P. A. *Macromolecules* **1992**, *25*, 1503.
(8) Borisov, O. V.; Birshtein, T. M.; Zhulina, E. B. *Modern Problems of Physical Chemistry of Macromolecules*; Center of Biological Research: Puschino, USSR, 1991; p 85.
(9) Misra, S.; Mattice, W. L.; Napper, D. H. *Macromolecules* **1994**, *27*, 7090.
(10) Zhulina, E. B. *Macromolecules* **1993**, *26*, 6273.
(11) Marko, J. F.; Rabin, Y. *Macromolecules* **1992**, *25*, 1503.
(12) Wittmer, J.; Joanny, J. F. *Macromolecules* **1993**, *26*, 2691.
(13) *Stealth Liposomes*; Lasic, D., Martin, F., Eds.; CRC Press: Boca Raton, 1995.
(14) Pincus, P. A. *Macromolecules* **1977**, *10*, 210.
(15) Alexander, S. *J. Phys. France* **1977**, *38*, 983.
(16) De Gennes, P.-G. *Macromolecules* **1981**, *14*, 1637.
(17) De Gennes, P.-G.; Pincus, P.; Velasco, R. M.; Brochard, F. *J. Phys. France* **1976**, *37*, 1461.
(18) Khokhlov, A. R.; Khachaturian, K. A. *Polymer* **1982**, *23*, 1742.
(19) Note that the same power law dependence for monomer density profile applies for $x \ll R_0$ in the case of random orientation of grafted polyions; however, in the latter case, an additional factor, $(1 - x^2/R_0^2)^{1/2}$, important at $x \leq R_0$, appears.
(20) Actually, at $h \cong R_0$, the orientation of polyions in the radial direction is sufficiently strong that their dimension in the axial direction is much smaller than R_0; thus, real (geometrical) overlapping of grafted polyions occurs at much smaller axial separation. See corresponding discussion for the planar brush in ref 5.
(21) Zhulina, E. B.; Birshtein, T. M. *Polym. Sci. USSR* **1985**, *27*, 570.
(22) Borisov, O. V. *J. Phys. II*, in press.
(23) Alexander, S.; Chaikin, P. M.; Grant, P.; Morales, G. J.; Pincus, P. A.; Hone, D. *J. Chem. Phys.* **1984**, *80*, 5776.
(24) Daoud, M.; Cotton, J. P. *J. Phys. France* **1982**, *43*, 531.
(25) Birshtein, T. M.; Zhulina, E. B. *Polymer* **1984**, *25*, 1453.
(26) Misra, S.; Varanasi, S. *J. Colloid Interface Sci.* **1991**, *146*, 251.
(27) Israels, R.; Leermakers, F.; Fleer, G. J. *Macromolecules* **1994**, *27*, 3087.
(28) Liatskaya, Yu. V.; Leermakers, F. A. M.; Fleer, G. J.; Zhulina, E. B.; Birshtein, T. M. *Macromolecules* **1995**, *28*, 3562.

MA9515801